Journal of Polymers and the Environment
https://doi.org/10.1007/s10924-018-1220-9

ORIGINAL PAPER

Synthesis, Luminescence and Thermal Properties of PVA–ZnO–Al_2O_3 Composite Films: Towards Fabrication of Sunlight-Induced Catalyst for Organic Dye Removal

Mohammad Mizanur Rahman Khan[1] · Mansura Akter[1] · Md. Khairul Amin[1] · Muhammad Younus[1] · Nilave Chakraborty[1]

Abstract
Poly(vinyl alcohol) (PVA)–ZnO–Al_2O_3 composite films have been prepared by the addition of different compositions of ZnO and Al_2O_3 through solvent casting method. Fourier transform infrared spectroscopy (FTIR), ultraviolet–visible spectroscopy (UV–Vis) and photoluminescence spectroscopy (PL) spectra revealed the successful incorporation of ZnO and Al_2O_3 onto PVA and interactions among ZnO, Al_2O_3 and PVA molecules. PL data indeed showed the enhanced luminescence property of composite films compared with the PVA. Thermogravimetric analysis (TGA) data showed that thermal stability of PVA–ZnO–Al_2O_3 composite films could be greatly improved by the incorporation of ZnO and Al_2O_3 into the system. The glass transition temperature (T_g) were increased for the composite samples using ZnO and Al_2O_3. Differential scanning calorimetry (DSC) measurements revealed that the melting temperature (T_m) of PVA–ZnO–Al_2O_3 composite films are significantly higher (~ 12 to 25 °C) than PVA. The photocatalytic measurements exhibited better photocatalytic degradation ability of PVA–ZnO–Al_2O_3 composites over PVA. Such photocatalytic capacity makes the PVA–ZnO–Al_2O_3 composite films promising candidates for the removal of organic dyes for water purification.

Keywords PVA–ZnO–Al_2O_3 composite films · Synthesis · Photoluminescence property · Thermal stability · Photocatalytic activity

Introduction

Polymers and Polymer composites materials are promising scientific areas owing to their ability to fabricate unique properties like optical, opto-electronic, high dielectric constant for particular applications such as sensors, capacitors and photocatalysts [1–5]. Among the polymers, polyvinyl alcohol (PVA) has attracted extensive attention of researchers because of its good film-forming nature, nontoxicity, biodegradability, excellent mechanical properties and optical transparency [6–9]. Due to the easy processability, it has been widely investigated as a host matrix for different kind of nanofillers [10, 11]. PVA was also employed as a suitable polymeric substrate for the photocatalytic waste water treatment [8]. Generally, PVA film can be synthesized with interesting functionalities through solvent casting method [12]. Using such synthesis technique, researchers are introducing various dopant materials to prepare composites with PVA and modulate the properties, such as morphology, optical property, thermal stability, photocatalytic activity and so on. The use of metal oxides, such as In_2O_3, CuO, MgO and other metal-based materials, for instance, CaF_2 has also been found to affect on the physicochemical, morphological, optical, thermal and sensing property of PVA [6, 13–15]. Thus, the addition of metal oxides can play significant role to modify the properties of PVA for application purposes. In this framework, introduction of metal oxides (for instance, ZnO and Al_2O_3) onto PVA can be a good candidate for photocatalytic application; as such materials have been investigated extensively as visible-light photocatalysts for the organic dye removal [16, 17]. So far, different photocatalytic oxide materials such as ZnO, CuO, TiO_2, and Fe_2O_3 have been effectively used to degrade different dyes [16, 18–20]. However, very few researches can be found in the literature,

✉ Mohammad Mizanur Rahman Khan
mizan_su@yahoo.com

[1] Department of Chemistry, Shahjalal University of Science and Technology, Sylhet 3114, Bangladesh

Published online: 20 March 2018

where ZnO and Al_2O_3 were used alone onto PVA to modify the mechanical, structural, and bioactive properties along with their optoelectronic and sensor application [21–24].

Among the oxide materials, ZnO is promising for photostable UV absorbent and for its biocompatible, luminescence, electrical and electro-optical properties [4, 25]. Due to such unique characteristics of ZnO and also the modified zinc oxide (for instance, cesium-doped zinc oxide), it is considered to be an effective additive to modify the material properties of PVA [4]. More importantly, ZnO exhibits interesting functionalities due to its large exciton binding energy (60 meV) and large band gap energy (3.37 eV at room temperature) which makes it as a good choice of photocatalyst [16]. Thus, ZnO turned out to be a good photocatalyst mainly for two reasons: (i) it can enhance photocatalytic activity, and (ii) it is nontoxic and lacks of creation of the dangerous by-products [26, 27]. Similarly, Al_2O_3 also has unique physical and chemical properties and has been used as a photocalyst for the removal of various organic pollutants [17, 28]. In this context, the addition of ZnO and Al_2O_3 onto PVA to prepare PVA–ZnO–Al_2O_3 composites may be interesting for its dye degradation properties. Thus, it may be significant to confirm the incorporation as well as interaction of ZnO, Al_2O_3 onto PVA as this understanding is essential for both the theoretical and application point of view. To the best of our knowledge, there have been no reports on the synthesis of PVA–ZnO–Al_2O_3 composite films by the combined use of ZnO and Al_2O_3 to modify the optical, luminescence and thermal properties of PVA. Moreover, there has been no report in the literature for the degradation of organic dye from waste water using PVA–ZnO–Al_2O_3 composite films as a photocatalyst.

Furthermore, being enthused by the lack of information in the literature on PVA-based ZnO–Al_2O_3 composite materials and their photocatalytic applications, it could therefore be significant to develop PVA–ZnO–Al_2O_3 composite films. Here, we report a simple solvent casting method for the preparation PVA–ZnO–Al_2O_3 composite films at room temperature, and their photo-catalytic degradation of methylene blue (MB) under sunlight irradiation. The enhance photoluminescence and thermal properties of the prepared composites have also been reported in the present work.

Experimental

Materials

All the reagents were analytical grade. Polyvinylalcohol (PVA) ($M_w = 72,000$, Merck), zinc oxide (ZnO, purity 99.9979%), aluminum oxide (Al_2O_3, purity 99.997%), acetone [$(CH_3)_2CO$, ≥ 99.5%, Sigma-Aldrich], methylene blue (Merck) were used as received.

Synthesis of PVA–ZnO–Al_2O_3 Composite Films

A simple solvent casting method was adopted for the synthesis of PVA–metal oxides composite films [12]. A known amount (0.75 g) of PVA was dissolved in boiling water (15 mL) and stirred well to prepare polymer solution. The prepared solution was transferred to vacuum rotary evaporator for casting the solvent. Then, a desired amount of metal oxides (ZnO and Al_2O_3) solution was sonicated for 2 h in separate containers. The sonicated metal oxides were directly mixed with the aqueous PVA solution in a rotary evaporator (temperature: 80–90 °C and rotation speed 200 rpm min^{-1}) to evaporate the solvent. Finally, the solution was cast in a glass petri dish and dried at room temperature for 24 h. After removal of solvent, a uniform metal oxides dispersed PVA films were obtained. The prepared films are free from air bubbles and with regular and uniformly dispersed metal oxide particles. Eight different synthesis batches were prepared with eight different compositions of ZnO and Al_2O_3 with constant amount of PVA (5 wt%) as presented in Table 1. Different molar concentrations of metal oxides were used but mixed molar concentrations were kept constant to 1 M. These composite films were further used for characterization and application studies (Table 1).

Characterization

Transmission FTIR spectra of PVA and PVA–ZnO–Al_2O_3 composite films were recorded between 400 and 4000 cm^{-1} using Shimadzu FTIR prestige 21 spectrometer. All UV–Vis spectra were obtained on Shimadzu UV-1800 spectrometer with the range of 200–800 cm^{-1}. The photoluminescence (PL) measurements were performed at room temperature using on Shimadzu RF-3501pc spectrofluorometer. The thermal characteristics of PVA and composite film samples were determined by TGA and DSC. The TGA analysis was

Table 1 Synthesis identifiers and various compositions of Al_2O_3 and ZnO for the synthesis of PVA–ZnO–Al_2O_3 composite films are listed

Synthesis identifier	Al_2O_3 (g)	ZnO (g)	Product
PVA	–	–	PVA film
α	0.90	0.48	Composite film
β	1.05	0.36	Composite film
γ	1.20	0.244	Composite film
δ	1.35	0.122	Composite film
ε	0.48	0.90	Composite film
ζ	0.36	1.05	Composite film
η	0.244	1.20	Composite film
θ	0.122	1.35	Composite film

carried out by measuring the weight loss of sample against the change of temperature using a Shimadzu TGA-50 thermogravimetric analyzer. For the measurements, 4.0 mg of sample was heated maintaining the temperature range between 30 and 850 °C at a rate of 20 °C min^{-1} under N_2 gas atmosphere. DSC measurements were performed on a Shimadzu TA-60A instrument under nitrogen flow (20 mL min^{-1}) in the temperature range 30–250 °C. The heating as well as cooling rates were maintained with a rate of 10 °C min^{-1}.

Photocatalytic Experiments

We evaluated the photocatalytic ability of PVA and PVA–ZnO–Al_2O_3 composite films following the degradation of MB under sunlight irradiation. The experiments were carried out in a same day to ensure similar illumination power of sunlight on the samples. For measurement, the photocatalyst sample (50 mg) was suspended in MB solution ($C_0 = 5$ mg L^{-1}). To obtain absorption–desorption equilibrium between the photocatalyst and the organic dyes, the reaction system was magnetically stirred for 30 min in the dark place and afterwards placed for sunlight irradiation. The stirring was kept continued after subsequent sunlight irradiation to reach the photocatalyst particles suspended during the measurements. At certain time intervals of solar irradiation, the aliquots of the mixture were removed and centrifuged at 3000 rpm for 20 min to separate the solid photocatalyst. Once the centrifugation is completed, the supernatant was collected for UV–Vis measurements to observe the adsorption and degradation behavior of MB. The characteristic absorbance data of MB at 664 nm was used to assess the % of degradation. The degradation efficiency of the photocatalyst was calculated using the following equation [29]: Degradation efficiency (D(%))=$\{A(MB)_0 - A(MB)\}_t / A(RhB)_0 \times 100$. Where, $A(MB)_0$ and $A(MB)_t$ denote the absorbance of MB at 664 nm in the dark and under sunlight irradiation, respectively.

Results and Discussion

Interaction of Metal Oxides (ZnO, Al_2O_3) on PVA

FTIR Spectra and Identification

Figure 1 shows the FTIR spectra of the samples of PVA and PVA–ZnO–Al_2O_3 composite films collected from different synthesis batches, presented in Table 1. All the characteristic peaks (see Table 2) of PVA were observed in PVA film [6, 30]. In the PVA spectrum, a broad and strong absorption at 3000–3600 cm^{-1}, peaking at 3432 cm^{-1} were observed. Such peak corresponds to the symmetrical stretching vibration of

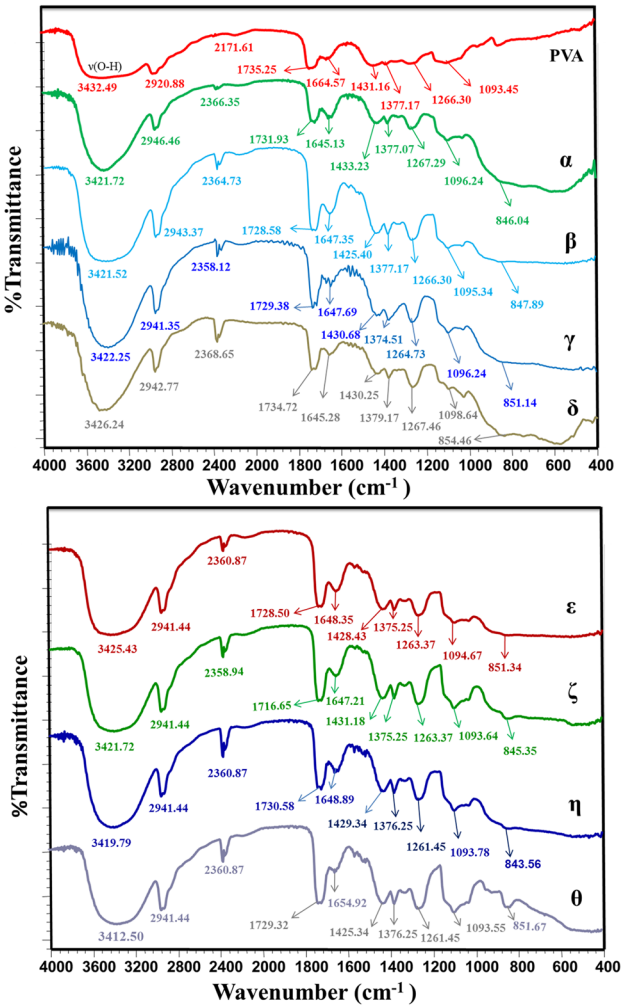

Fig. 1 FTIR spectra of PVA and PVA–ZnO–Al_2O_3 composite films obtained from different synthesis batches (α–θ). The syntheses were performed by the addition of different amount of ZnO and Al_2O_3 as presented in Table 1

O–H, originating from the intermolecular and intramolecular hydrogen bonds in PVA. The peak found at 2920 cm^{-1} is assigned to the C–H stretching vibrations of $–CH_2–$ skeleton. A strong band at 1093 cm^{-1} is assigned to stretching vibration of C–O in the C–O–H groups. The bands at 1431 and 1377 cm^{-1} are appeared for the bending and wagging vibrations of CH_2 groups respectively. The C–H wagging is seen at 1266 cm^{-1}.

The peaks found at 1735 and 1664 cm^{-1} is assigned to C=C stretching and C=O stretching, respectively. For all the samples of PVA–ZnO–Al_2O_3 composite films, the frequency of the symmetrical stretching vibration of hydroxyl group shifted to lower wave number (3346–3428 cm^{-1}) than that of PVA film, indicating slightly reduced hydrogen bonding among the PVA chains [31]. When metal oxides (ZnO and Al_2O_3) are interacted with the PVA matrix, they may form

Table 2 Characteristic FTIR peaks PVA and PVA–ZnO–Al_2O_3 composite films

Peak designation	Peak values of the corresponding samples (cm^{-1})								
	PVA	α	β	γ	δ	ε	ζ	H	θ
O–H stretching	3432	3421	3421	3423	3426	3421	3421	3419	3412
C–H stretching	2920	2946	2943	2941	2942	2941	2941	2941	2941
C=C stretching	1735	1731	1730	1729	1734	1728	1730	1730	1729
C=O stretching	1664	1645	1647	1647	1645	1648	1648	1647	1654
C–O stretching	1093	1096	1095	1096	1098	1094	1093	1093	1093
C–H wagging	1266	1267	1266	1264	1263	1263	1261	1261	1261
CH_2 bending	1431	1433	1425	1430	1430	1428	1429	1425	1425
CH_2 wagging	1377	1377	1377	1374	1379	1375	1376	1375	1376

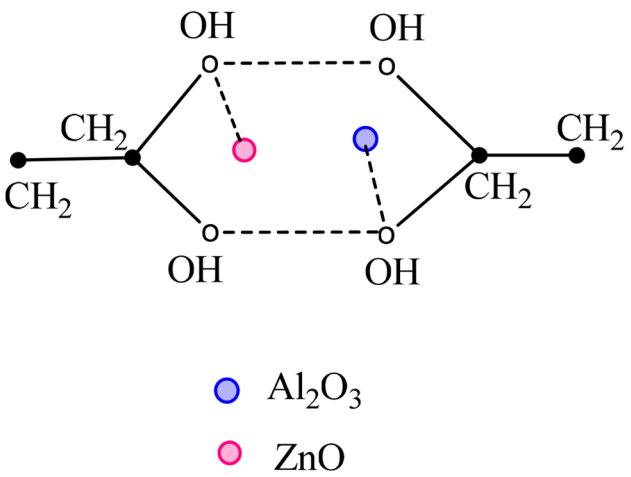

Fig. 2 Probable hydrogen bonds of ZnO and Al_2O_3 with PVA. Figure shows the lateral section of PVA molecule. The broken lines indicate the hydrogen bonds

bonds with the hydroxyl groups of PVA, which reduce the hydrogen bonding among PVA molecules. A possible interaction of ZnO and Al_2O_3 with the PVA molecules is shown in Fig. 2:

Furthermore, the characteristics peak of metal oxides (ZnO and Al_2O_3) at 843–851 cm^{-1} appears in the FTIR spectra of all PVA–ZnO–Al_2O_3 composite samples. Similar peak of ZnO and Al_2O_3 was also observed by other researchers [32, 33]. Thus FTIR results confirm the incorporation of ZnO and Al_2O_3 in the PVA matrix and their interaction with PVA molecules.

UV–Vis Spectra and Identification

The interaction of PVA with metal oxides (ZnO and Al_2O_3) in composite films and their optical band gap were estimated by UV–Vis spectroscopy as presented in Fig. 3 (a, b and c). In the case of PVA film, the characteristics absorption bands observed around at 200–240 nm, is assigned to the carbonyl-groups associated with ethylene unsaturation of the type –$(CH{=}CH)_2$ CO–[34]. The weaker and the shoulder form of this band are due to the presence of isolated carbonyl groups [35]. The bare metal oxides, ZnO and Al_2O_3 showed absorption bands around at 272 nm and a shoulder band around at 348 nm. Similar absorption bands for ZnO and Al_2O_3 was reported in references [36, 37]. For the composite films, absorption spectra were observed around at 379 nm for the intrinsic band-gap absorption of transition metal oxides corresponds to the electron transitions from the valence band to the conduction band [38]. Such peak indicates a bathochromic shift or red shift of PVA and implies the strong interactions between PVA and metal oxides (ZnO and Al_2O_3). Such kind of absorption peaks due to the interaction of metal oxides with PVA was also previously reported in reference [21]. Concerning the optical band gap estimation of the samples, we observed the characteristic absorption maxima of metal oxides (ZnO–Al_2O_3) and PVA–ZnO–Al_2O_3 composite films in the range of 377–380 nm. The optical band gaps of all the samples were obtained from the absorption maxima using the band-gap equation ($E = hc/\lambda$, where E, h, c, and λ represent the band-gap energy, Planck's constant, the velocity of light, and the wavelength of absorption maxima, respectively). The optical band gap of the PVA–ZnO–Al_2O_3 composite samples and bare ZnO–Al_2O_3 were observed in the range of 3.26–3.29 and 4.46 eV, respectively. In PVA–ZnO–Al_2O_3 composites, it can be seen that the addition of different amounts of ZnO and Al_2O_3 can significantly affect the absorption of light. When ZnO and Al_2O_3 were added onto the PVA, the absorption maxima decreases intensely in the visible region due to shielding of light absorption by PVA matrix. Similar shielding of light absorption was previously observed for graphene–ZnO composite materials [39]. Finally, based on the above results, it is assumed that the photocatalytic absorption and degradation ability of bare ZnO–Al_2O_3 are better than it's composites with PVA. However, the addition of ZnO and Al_2O_3 may able to improve the photocatalytic performance of PVA–ZnO–Al_2O_3 composite films than PVA alone.

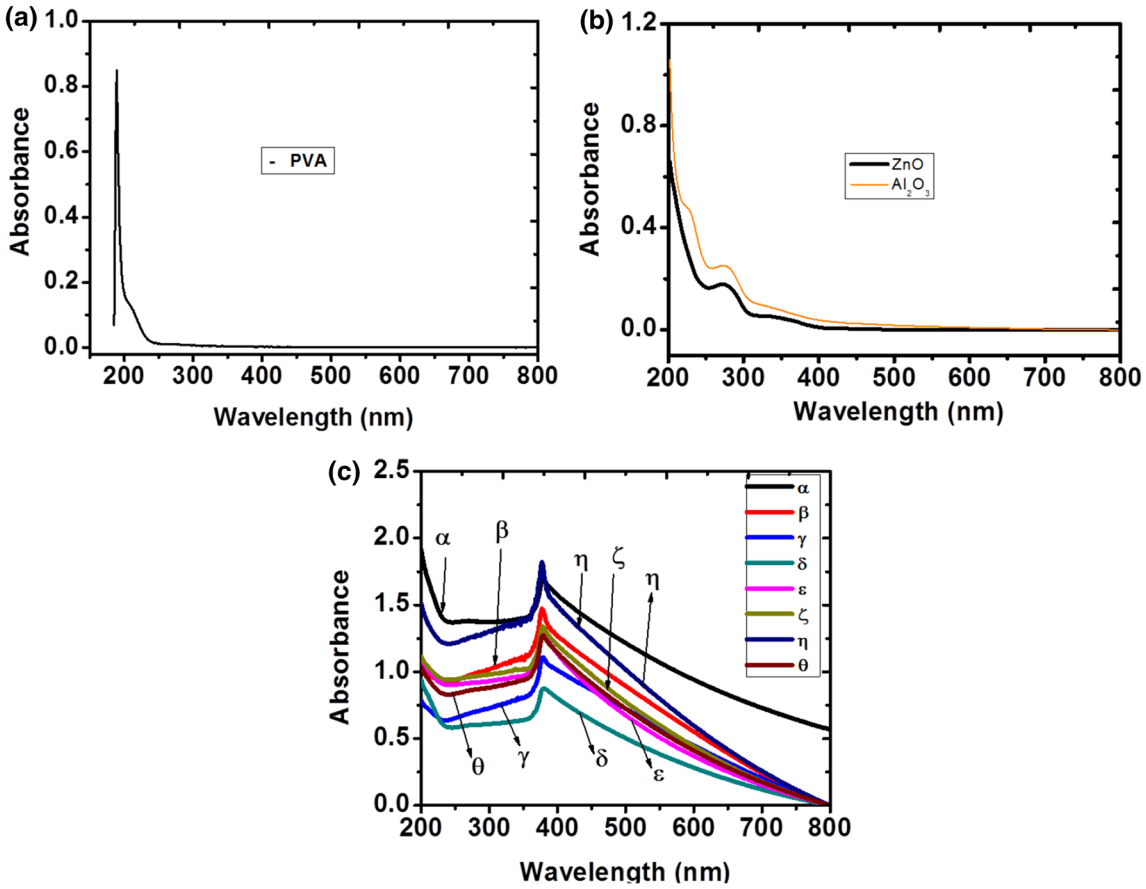

Fig. 3 UV–Vis spectrum of **a** PVA, **b** ZnO, Al_2O_3 and **c** PVA–ZnO–Al_2O_3 composite films (α–θ)

Photoluminescence Property

The interaction among ZnO, Al_2O_3 and PVA in PVA–Al_2O_3–ZnO composites can be further confirmed by PL measurements. Figure 4 represents the room temperature PL spectra of PVA–Al_2O_3–ZnO composite films with different Al_2O_3 and ZnO ratio at excitation wavelength 378 nm. A sharp UV emission (320–400 nm) is observed for pure PVA (inset a of Fig. 4) which is corresponded to $\pi^* \rightarrow$ n electronic transition of the –OH groups for isotactic, syndiotactic and atactic configurations of PVA, originating from stereo-regularity of the –OH groups [15, 21, 22]. A red shifting of peak emission compared to PVA is seen for all the composite film samples, which exhibits broadband blue emission (420–440 nm) (inset b of Fig. 4). This observation reveals the incorporation of ZnO and Al_2O_3 into PVA matrix as well as rearrangement of delocalized n-electrons of –OH groups in PVA. The broad blue emission in the composites may be related to the different deep level transitions like zinc interstitial, $Zn_i \rightarrow$ zinc vacancy, V_{Zn} and/or conduction band, CB$\rightarrow$ zinc vacancy, V_{Zn} in ZnO [15, 21, 31, 40]. Looking at the PL spectra, it is evident that the intensity depends upon

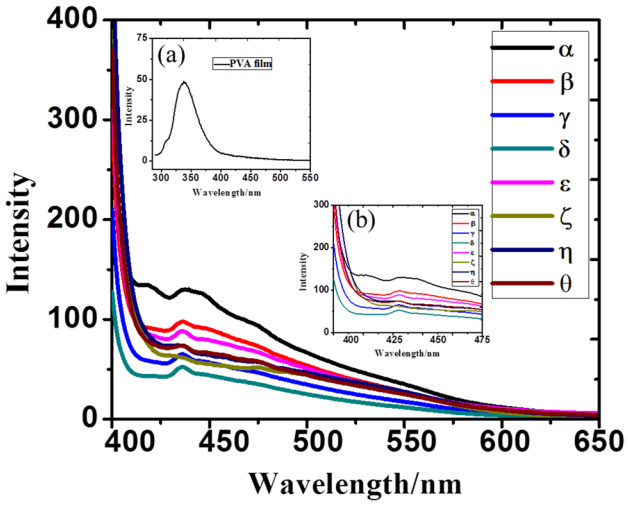

Fig. 4 PL spectra of PVA (inset **a**) and PVA–Al_2O_3–ZnO composite films. Inset **b** represents the magnified PL spectra of corresponding PVA–Al_2O_3–ZnO composite samples to identify more clearly the intensity dereferences among them

the amount of Al_2O_3 and ZnO in the composites. A maximum PL emission was found for the composite of samples α. The PL intensity decreases linearly (α→ δ) with the increasing of Al_2O_3 content and decreasing of ZnO content (Fig. 4) in the composites. So, there is a possibility of generating nonradiative recombination centers with the increase of Al content in the composite samples which renders the intensity of PL [41]. Besides, the n-type ZnO can trap electrons and permits more holes to recombine through the interface of PVA and ZnO, thus enhanced luminescence is attained. An opposite trend is realized with the addition of excess ZnO (ε–θ). Such behavior may due to the blocking of most of the electrons around ZnO surface that restricts the recombination process of the composites [42, 43]. The above results indicate that the synthesized PVA–Al_2O_3–ZnO composite films can be a promising candidate for light-emitting diode, solar cell, laser, and sensor [15, 23, 24].

Thermal Properties

The TGA thermograms of PVA and PVA–ZnO–Al_2O_3 composite films are presented Fig. 5 and the corresponding thermal degradation properties are listed in Table 3. We observed a three-step decomposition process for both PVA and PVA–ZnO–Al_2O_3 composite films, demonstrating the three separate stages of weight loss at their corresponding degradation temperature range under nitrogen atmosphere. The first decomposition step was noticed at 93–179 °C and 50–179 °C and the corresponding weight loss was found 4 and 0.4–2% for PVA and PVA–ZnO–Al_2O_3 composite samples, respectively due to the loss of moisture and partial dehydration of PVA chains [6, 44].

For PVA, the second degradation step was identified at 291–382 °C and the weight loss is 31%. However, at the second step of PVA–ZnO–Al_2O_3 composite films, the mass loss was observed 9.2–20% in the temperature range 227–361 °C. Such degradation step can be attributed to

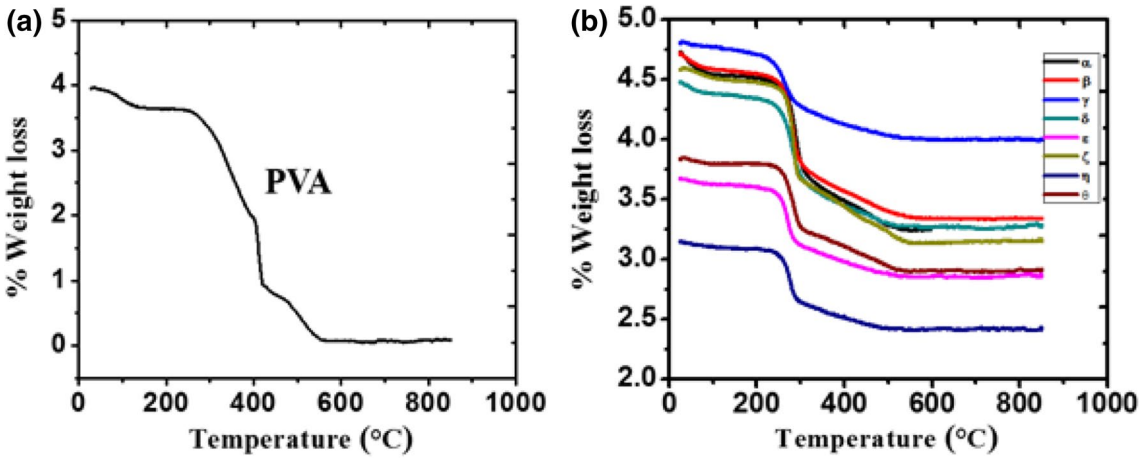

Fig. 5 TGA curves of **a** PVA and **b** PVA–ZnO–Al_2O_3 composite films (α–θ)

Table 3 Decomposition temperature and % of weight loss of PVA and PVA–ZnO–Al_2O_3 composite films obtained from TGA analysis. The samples, decomposition temperature and % of weight loss for different degradation steps are listed

Samples	Temperature (T) and % of weight loss (WL) at three decomposition steps					
	First step		Second step		Third step	
	T (°C)	WL (%)	T (°C)	WL (%)	T (°C)	WL (%)
PVA	93–179	4	291–382	31	485–608	13
A	58–125	2	334–361	20	458–620	2.3
B	62–141	1.3	245–354	17	493–614	1.5
Γ	79–179	1.1	227–334	9.2	489–626	1.1
Δ	50–151	1.6	236–346	16.6	509–614	0.4
E	75–165	0.8	244–335	13	488–613	1
Z	92–175	0.8	245–348	19	514–614	1
H	65–152	0.9	245–334	14	452–565	1.8
Θ	73–160	0.4	244–350	15	482–634	1.8

the heating arrangement of the polymer structure [45]. Certainly, the major weight loss was found at this second step both for PVA and PVA–ZnO–Al_2O_3 composite films. However, weight loss is much lower for composite samples compared to PVA indicating the more thermal stability nature of composite films. These results are consistent with the previous report for the synthesis of PVA–metal oxide composites [6]. The third decomposition step was occurred at 485–608 °C and 452–634 °C and the corresponding weight losses were recognized 13% and 0.4–2.3% for PVA and PVA–ZnO–Al_2O_3 composite films, respectively. The weight loss observed for such step may correspond to the further degradation of polymer structure which subsequently undergoes decomposition forming carbonaceous matter and remains constant subsequently showing the plateau behavior [46].

Comparing the samples for all three decomposition steps, we observed that the addition of ZnO and Al_2O_3 had significantly influenced on the % of weight loss of PVA (Table 3). The observed improved thermal stability may be for interactions between PVA and metal oxides (ZnO and Al_2O_3). The interactions between PVA and metal oxides (ZnO and Al_2O_3) may cause the slow degradation process, and restrict the motions of polymer chains, thus decrease the weight loss of PVA [47]. Similar interactions between metal oxides and polymer, as a result of improvement of the thermal stability nature were reported in reference [48]. However, among all the PVA–ZnO–Al_2O_3 composite samples (α–θ), no significant difference of the % of weight loss was observed, although the sample γ and α had experienced slightly lower and higher weight loss, respectively at the second stage. This result indicates the higher and lower thermal stability nature of the samples γ and α respectively compare to other composite samples.

DSC curves of PVA and PVA–ZnO–Al_2O_3 composite films (α to θ) are shown in Fig. 6. The cooling cycle behavior is shown in above of the heating cycle of each sample. During heating cycle, PVA shows three endothermic peaks, whereas PVA–ZnO–Al_2O_3 composite films exhibit different thermal response with two distinct characteristic features as a function of temperature. The first endothermic step observed at 48.11 and 39–75.55 °C for PVA and PVA–ZnO–Al_2O_3 composite films respectively is attributed to the glass transition temperature (T_g). The glass transition temperature of PVA is generally occurs at 86 °C, however in our case occurred at about 48.11 °C due to the presence of moisture [49]. The incorporation of metal oxides (ZnO and Al_2O_3) in the PVA matrix increases the Tg value in the range of 8.89–18.55 °C for the composite samples of α–η, along with a higher energy requirement as seen from the clear peak like shape of glass transition. Only the exception was observed for the samples β and θ, where the T_g value decreases by 9.11 °C for β and almost same for θ compared to PVA. Similar results are also observed in reference [6]. It is well-known that glass transition process is influenced by molecular packing, chain rigidity and linearity. The increase of T_g value with the incorporation of ZnO and Al_2O_3 for the composite samples (except β and θ) may be because of the strong interactions between the PVA and the metal oxides (ZnO and Al_2O_3). Such intercalations cause a decrease in mobility of polymer chains which lead to the variation of the glass transition temperature. The observed increase in T_g of the PVA is very similar to the results mentioned in literature [46]. The second endothermic peak observed at 76.38 and 83 °C for PVA and the sample β respectively is attributed to removal of free (moisture) as well as hydrogen bonded water [50]. Similar kind of peak was reported for PVA and PVA–metal oxide composites [6]. We also found exothermic

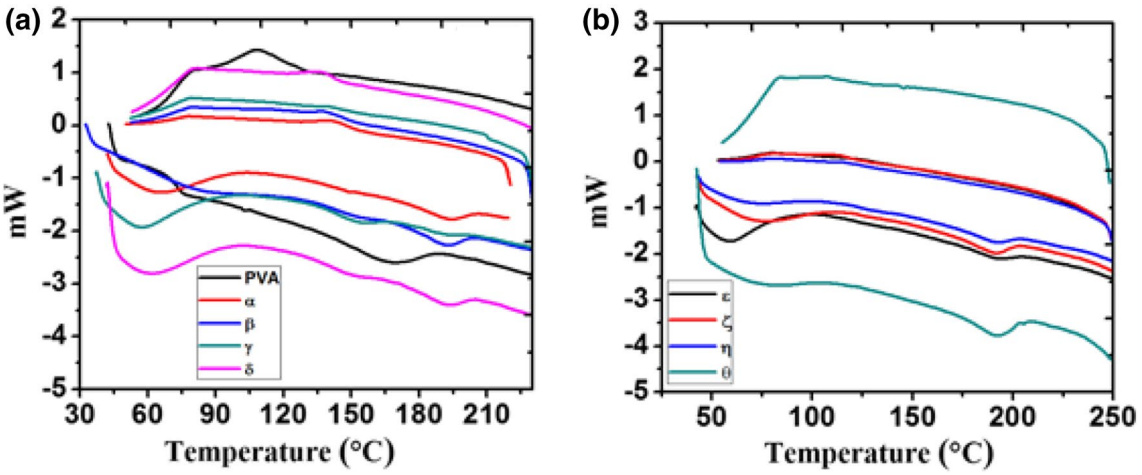

Fig. 6 DSC thermograms of **a** PVA and **b** PVA–ZnO–Al_2O_3 composite films obtained from different synthesis batches (α–θ). The thermograms were recorded during both heating and cooling cycles. The cooling cycle behavior are shown in above of the heating cycle of the same materials

peak in the thermograms recorded during the cooling cycle (Fig. 6). The third endothermic peak in the DSC thermogram around at 170 °C for PVA corresponds to the melting temperature (T_m) of PVA. Similar endothermic peak (melting temperature) was identified in the range of 192–195 °C for the composites (Table 4). It is clear that PVA–ZnO–Al_2O_3 composite films melt significantly at higher temperature (~ 12 to 25 °C) as compared to PVA. A similar trend of increase in the melting temperature has been observed in cellulose nanocrystals doped PVA [51], metal salts/metal/metal oxide added PVA [46], and PVA–iron oxide nanocomposites [52]. However, among the PVA–ZnO–Al_2O_3 composite samples (α–θ), no significant difference of the melting temperature was identified.

The increase in T_m of the composite samples may be for the increase in the crystallinity of the sample. PVA is considered to be crystallized as a result of arrangement of polymer chains in an ordered fashion to each other. The addition of ZnO–Al_2O_3 in PVA matrix may cause strong interaction of polymer chains with the metal oxide surface, which may facilitate to align polymer chains in an ordered manner. Such alignment and crystallization of the polymer chains within the individual PVA films enhanced the melting temperature of composite samples [7]. Besides, the crystallinity of PVA in the composite films may increase due to the interactions between the main chain of PVA and the metal oxides (see FTIR discussion). Thus, the heat resistance of the PVA–ZnO–Al_2O_3 composite films increases, leading to increase of the melting temperatures [51]. Thus it can be concluded that the combined addition of ZnO and Al_2O_3 increases the thermal stability of all prepared PVA–ZnO–Al_2O_3 composite films. Similar observation of the improved thermal stability of composites was reported by doping nano aluminium oxide and zinc oxide in poly (methyl methacrylate) [46].

The degree of crystallinity of all prepared samples was calculated using the following equation [6]:

$$\text{Degree of crystallinity} = \frac{\Delta H_m}{\Delta H_m^\circ} \times 100$$

where ΔH_m is the measured enthalpy of melting from the DSC thermogram and ΔH_m° is the enthalpy of melting for 100% crystalline PVA (ΔH_m° is 138.6 J g^{-1}) [6, 53]. The value of melting enthalpy for PVA is 20.29 J g^{-1} and such value decreases from 0.92 to 6.68 J g^{-1} for composite samples indicating decrease in crystallinity. The calculated degree of crystallinity of all samples is listed in Table 4. The crystallinity of PVA was found 14.64%, whereas for the composite samples (α–θ) the crystallinity lies in the range of 0.66–4.82%. Similar kind of decrease in crystallinilty with the addition of metal oxides with PVA was reported in references [6, 52, 53].

Table 4 Effect of heating–cooling cycles on the thermal properties of PVA–ZnO–Al_2O_3 composite films and their calculated crystallinity

Sample	T_g (peak) (°C)	T_m (peak) (°C)	ΔH_m (J g^{-1})	Crystallinity (%)
PVA	48.1	170.0	20.29	14.64
α	65.7	194.4	5.95	4.29
β	39.0	193.1	6.46	4.66
γ	57.0	182.1	0.92	0.66
δ	59.6	193.7	4.81	3.47
ε	58.5	194.7	3.95	2.85
ζ	75.6	191.7	6.67	4.81
η	71.9	193.3	4.56	3.29
θ	48.0	192.6	6.68	4.82

Photocatalytic Activity

The photocatalytic ability of the ZnO–Al_2O_3, PVA and PVA–ZnO–Al_2O_3 composite films was identified by observing the photodegradation of organic dye (MB) under sunlight irradiation. For instance, the time dependent UV–Vis absorption spectra of MB are shown in Fig. 7, where the photocatalytic activities of bare ZnO–Al_2O_3, PVA and the composite samples of α and ε toward MB are presented. The changes in the absorption spectra of MB state the change in concentration of respective sample. If the absorption spectra decrease apparently, it demonstrates an effective adsorption of MB on the composites. It is clear from Fig. 7 b and c that there is obvious decrease in the absorption maxima for samples α and ε and the absorption maximum decreased gradually with an appreciable blue shift and it finally reached zero after 240 min of irradiation. However, there is no significant variation of absorption maximum was seen between the two composite samples, only slight difference of absorption maximum was observed after 30 and 60 min of irradiation. The blue shift in the absorption maxima of the samples indicates the gradual adsorption of MB to the samples leading to its complete degradation. Similar degradation phenomenon of MB using different catalysts was previously reported by other researchers [54]. Such gradual degradation of MB was confirmed by color changes in reaction mixture from blue to light blue with absorption band shift from 664 to 616 nm. Additionally, on continued irradiation of sunlight, the solution color changed into colorless which confirms the complete degradation of organic dye from its conjugated structure.

We observed that in the absence of the photo-catalyst, the degradation of MB is hardly occurred (only about 2%) on sunlight irradiation. In the presence of bare ZnO–Al_2O_3, after a time span of only 10 min, 96% degradation of MB is realized, this gradually reached 100% after 30 min irradiation. This demonstrates that metal oxides ZnO–Al_2O_3 have

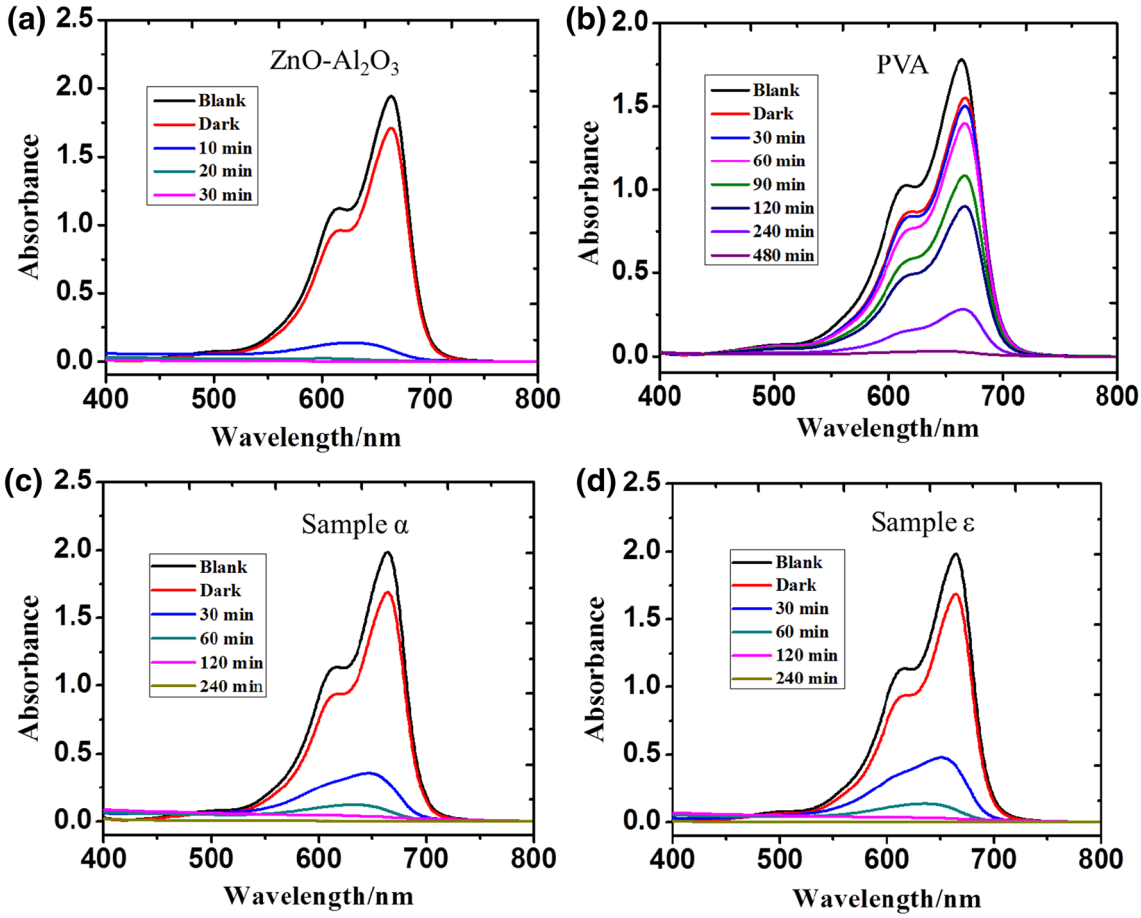

Fig. 7 Changes in the UV–Vis absorption spectra of MB aqueous solution in the presence of **a** ZnO–Al_2O_3, **b** PVA film, **c** PVA–ZnO–Al_2O_3 (sample α), and **d** PVA–ZnO–Al_2O_3 composite films (sample ε)

excellent photocatalytic ability under sunlight. However, PVA–ZnO–Al_2O_3 composite films exhibited comparatively lower and higher degree of photocatalytic degradation ability than bare ZnO–Al_2O_3 and PVA, respectively; it took 120 min for the complete degradation. In case of PVA film, complete degradation of MB occurs after 480 min. Such results prove that ZnO–Al_2O_3 itself have higher degradation ability than PVA–ZnO–Al_2O_3 composites and are able to significantly increase the photocatalytic performance of its composites with PVA. This may be explained as follows: ZnO–Al_2O_3 significantly interact with the PVA matrix and weaken the intermolecular hydrogen bonding among the polymer chain (see FTIR discussion). When the ZnO–Al_2O_3 incorporate to the PVA matrix, a layer may formed in the surface of ZnO–Al_2O_3 structure and this shields the light from the surface of the PVA–ZnO–Al_2O_3 composite films, reducing the photo absorption of ZnO–Al_2O_3 and thus decreasing the photocatalytic degradation ability [41]. The mechanism of the photocatalytic degradation process for the PVA–ZnO–Al_2O_3 composite films can be clarified as follows:

Under sunlight ($h\upsilon$) irradiation, ZnO and Al_2O_3 are excited to generate electrons–holes pairs which are powerful oxidizing and reducing agents, respectively.

$$ZnO + h\upsilon \rightarrow h^+ + e^- \text{and} \, Al_2O_3 + h\upsilon \rightarrow h^+ + e^-$$

The photo generated holes, then react directly with the organic pollutants (MB) or with surrounding water molecules to generate hydroxyl radicals (primary oxidant). At the same time the photo generated electrons subsequently react with surrounding water and oxygen molecules to generate hydroxyl and superoxide radicals. The presence of oxygen can prevent the re-combination of hole–electron pairs. The oxidative and reductive reactions are expressed as follows:

$$OH^- + h^+ \rightarrow \cdot OH \, \text{and} \, O_2 + e^- \rightarrow O_2^-$$

For a complete reaction, the final products of the reaction are CO_2 and H_2O [54]:

$$MB + \cdot OH \rightarrow \text{products} \left(CO_2 + H_2O\right)$$

When ZnO–Al_2O_3 incorporates into the PVA structure, the polymer layer may restrain the adsorption of the MB

molecules on the surface of catalysts reaction and lower the photocatalytic degradation. Thus it may be concluded that although the photocatalytic ability is different for composites and metal oxides, however, both of them can be substantially used for the removal of organic dye for water purifications.

Conclusions

Poly(vinyl alcohol) (PVA)–ZnO–Al_2O_3 composite films have been successfully prepared by the addition of different compositions of ZnO and Al_2O_3 using a simple solvent casting method. The data obtained by FTIR measurement show the possible incorporation of metal oxides (ZnO and Al_2O_3) in PVA. The interaction of metal oxide with PVA is further confirmed by the UV–Vis measurements, indicating the bathochromic shift of the absorption peaks of composite samples. Such strong host polymer and metal oxides interactions were also supported through PL studies, where the enhanced luminescence property of composite films was observed compared with the PVA. The thermal stability of PVA–ZnO–Al_2O_3 composite films was greatly improved by the incorporation of ZnO and Al_2O_3 into the system. The glass transition temperature (T_g) were increased for the composite films compared to PVA. DSC measurement also revealed the higher melting temperature (Tm) (~ 22 to 25 °C) of the PVA–ZnO–Al_2O_3 composite films than PVA. The photocatalytic measurement demonstrates that PVA–ZnO–Al_2O_3 composite films have the better degradation ability of MB than PVA.

All of the data are direct evidence that, the luminescence and thermal properties of the PVA–ZnO–Al_2O_3 composite films can be improved by using together ZnO and Al_2O_3. Moreover, the photocatalytic performance indicates that PVA–ZnO–Al_2O_3 composite films can be promising candidates for the removal of organic dyes for water purification.

Acknowledgements The authors gratefully acknowledge Organic and Materials Chemistry Laboratory of the Chemistry Department, SUST for supporting experimental works.

References

1. Zhang X-J, Wang G-S, Wei Y-Z, Guo L, Cao M-S (2013) Polymer-composite with high dielectric constant and enhanced absorption properties based on graphene–CuS nanocomposites and polyvinylidene fluoride. J Mater Chem A 1:12115–12122
2. Rao Y, Wong CP (2004) Material characterization of a high-dielectric-constant polymer–ceramic composite for embedded capacitor for RF applications. J Appl Polym Sci 92:2228–2231
3. Rao Y, Ogitani S, Kohl P, Wong CP (2002) Novel polymer–ceramic nanocomposite based on high dielectric constant epoxy formula for embedded capacitor application. J Appl Polym Sci 83:1084–1090
4. Kundachira Subramani N(2015) Opto-electrical characteristics of poly(vinyl alcohol)/cesium zincate nanodielectrics. J Phys Chem C 119(35):20244–20255
5. Suma GR, Subramani NK, Sachhidananda S, Satyanarayana SV, Siddaramaiah (2017) J Mater Sci: Mater Electron. https://doi.org/10.1007/s10854-017-7148-3
6. Singhal A, Kaur M, Dubey KA, Bhardwaj YK, Jain D, Pillai CGS, Tyagi AK (2012) Polyvinyl alcohol–In_2O_3 nanocomposite films: synthesis, characterization and gas sensing properties. RSC Adv 2:7180–7189
7. Jia YT, Gong J, Gu XH, Kim HY, Dong J, Shen XY (2007) Fabrication and characterization of poly (vinyl alcohol)/chitosan blend nanofibers produced by electrospinning method. Carbohydr Polym 67:403–409
8. Jung G, Kim H-II (2014) Synthesis and photocatalytic performance of PVA/TiO_2 graphene-MWCNT nanocomposites for dye removal. J Appl Polym Sci 40715:1–7. https://doi.org/10.1002/APP.40715
9. Shilpa KN, Subramani NK, Sachhidanand S, Madhukar BS, Siddaramaiah (2016) Visibly transparent PVA/sodium doped dysprosia ($Na_2Dy_2O_4$) nano composite films, with high refractive index: an optical study. J Alloys Compd 694:884–891
10. Kumar RV, Koltypin Y, Cohen YS, Aurbach D, Palchik O, Felner I, Gedanken A (2000) Preparation of amorphous magnetite nanoparticles embedded in polyvinyl alcohol using ultrasound radiation. J Mater Chem 10:1125–1129
11. Qian XF, Jin J, Huang JC, Yang YF, Guo XX, Zhu ZK (2001) The preparation and characterization of PVA/Ag_2S nanocomposite. Mater Chem Phys 68:95–97
12. Lagashetty A, basavaraj S, Bedre M, Venkatarman A (2009) Metal oxides dispersed polyvinyl alcohol nanocomposites. J Metall Mater Sci 51:297–306
13. Dey KK, Kumar P, Yadav RR, Dhar A, Srivastava AK (2014) CuO nanoellipsoids for superior physicochemical response of biodegradable PVA. RSC Adv 4:10123–10132
14. Karthikeyan K, Poornaprakash N, Selvakumar N, Jeyasubrmanian K (2009) Thermal properties and morphology of MgO-PVA nanocomposite film. J Nanostruct Polym Nanocompd 5:83–88
15. Nakhaei O, Shahtahmassebi N, Rezaeeroknabadi M, Mohagheghi MMB (2012) Synthesis, characterization and study of optical properties of polyvinyl alcohol/CaF_2 nanocomposite films. Sci Iranica 19:1979–1983
16. Anbuvannan M, Ramesh M, Viruthagiri G (2015) Synthesis, characterization and photocatalytic activity of ZnO nanoparticles prepared by biological method. Spectrochim Acta A. https://doi.org/10.1016/j.saa.2015.01.124
17. Pathania D, Katwal R, Kaur H (2016) Enhanced photocatalytic activity of electrochemically synthesized aluminum oxide nanoparticles. Int J Miner Metall Mater 23:358–371
18. Khodja AA, Sehili T, Pilichowski J-F, Boule P (2001) Photocatalytic degradation of 2-phenylphenol on TiO_2 and ZnO in aqueous suspensions. J Photochem Photobiol A 141:231–239
19. Umadevi M, Christy AJ (2013) Synthesis, characterization and photocatalytic activity of CuO nanoflowers. Spectrochim Acta A 109:133–137
20. Valenzuela MA, Bosch P, Jiménez-Becerrill J, Quiroz O, Páez AI (2002) Preparation, characterization and photocatalytic activity of ZnO, Fe_2O_3 and $ZnFe_2O_4$. J Photochem Photobiol A 148:177–182
21. Fernandes DM, Hechenleitner AW, Lima SM, Andrade LH, Caires AR, Pineda EG (2011) Preparation, characterization, and photoluminescence study of PVA/ZnO nanocomposite films. Mater Chem Phys 128:371–376
22. Aga Mu (2010) Doping of polymers with zno nanostructures for optoelectronic and sensor applications. Nanowires Science and Technology. Intech, Rijeka

23. Sugumaran S, Bellan CS, Nadimuthu M (2015) Characterization of composite PVA–Al_2O_3 thin films prepared by dip coating method. Iran Polym J 24:63–74
24. Samzadeh-Kermani A, Mirzaee M, Ghaffari-Moghaddam M (2016)Polyvinyl alcohol/polyaniline/ZnO nanocomposite: synthesis, characterization and bactericidal property. Adv Biol Chem 6:1–11
25. Subramani NK, Shilpa KN, Shivanna S, Siddaramaiah H (2016) Highly flexible and visibly transparent poly(vinyl alcohol)/calcium zincate nanocomposite films for UVA shielding applications as assessed by novel ultraviolet photon induced fluorescence quenching. Macromolecules 49(7):2791–2801
26. Sakthivel S, Nepolian B, Shankar MV, Palanichamy M, Arabindoo B, Murugesan V (2003) Solar photocatalytic degradation of azo dye: comparison of photocatalytic efficiency of ZnO and TiO_2. Energy Mater Sol Cells 77:65–82
27. Qunitana M, Ricra E, Rodriguez J, Estrada W (2002) Spray pyrolysis deposited zinc oxide films for photo-electrocatalytic degradation of methyl orange: influence of the pH. Catal Today 76:141–148
28. Anderson C, Bard AJ (1997) Improved photocatalytic activity and characterization of mixed TiO_2/SiO_2 and TiO_2/Al_2O_3 materials. J Phys Chem B 101:2611–2616
29. Reddy DA, Lee S, Choi J, Park S, Ma R, Yang H, Kim TK (2015) Green synthesis of AgI-reduced graphene oxide nanocomposites: toward enhanced visible-light photocatalytic activity for organic dye removal. Appl Surf Sci 341:175–184
30. Akhter S, Allan K, Buchanan D, Cook JA, Campion A, White JM (1988) XPS and IR study of X-ray induced degradation of PVA polymer film. Appl Surf Sci 35:241–258
31. Jiang L, Shen XP, Wu JL, Shen KC (2010) Preparation and characterization of graphene/poly(Vinylalcohol) nanocomposites. J Appl Polym Sci 118:275–279
32. Kazeminezhad I, Sadollahkhani A, Farbod M (2013) Synthesis of ZnO nanoparticles and flower-like nanostructures using nonsono- and sono-electrooxidation methods. Mater Lett 92:29–32
33. Varghese N, Hariharan M, Cherian AB, Sreenivasan PV, Paul J, Antony AK A (2014) PVA-assisted synthesis and characterization of nano α-alumina. Int J Sci Res Publ 4:1–5
34. Rao NR (1967) Ultraviolet and visible spectroscopy. Chemical applications, Butterworth, London
35. Jayasekaro R, Harding I, Bowater I, Christie GBY, Lonergan GT (2004) Preparation, surface modification and characterisation of solution cast starch PVA blended films. Polym Test 23:17–27
36. Segets D, Gradl J, Taylor RK, Vassilev V, Peukert W (2009) Analysis of optical absorbance spectra for the dDetermination of ZnO nanoparticle size distribution, solubility, and surface energy. ACS Nano 3(7):1703–1710
37. Prashanth PA, Raveendra RS, Hari Krishna R, Ananda S, Bhagya NP, Nagabhushana BM, Lingaraju K, Raja Naika H (2015) J Asian Ceram Soc. https://doi.org/10.1016/j.jascer.2015.07.001
38. Zak AK, Razali R, Majid WHA, Darroudi M (2011) Synthesis and characterization of a narrow size distribution of zinc oxide nanoparticles. Int J Nanomed 6:1399–1403
39. Bu Y, Chen Z, Li W, Hou B (2013) Highly efficient photocatalytic performance of Graphene–ZnO quasi-shell-core composite material. ACS Appl Mater Interface 5:12361–12368
40. Djurišić AB, Leung YH, Tam KH, Ding L, Ge WK, Chen HY, Gwo S (2006) Green, yellow, and orange defect emission from ZnO nanostructures: Influence of excitation wavelength. Appl Phys Lett 88:103107
41. Zhou J, Sun G, Zhao H, Pan X, Zhang Z, Fu Y, Mao Y, Xie E (2015) Tunable white light emission by variation of composition andde fects of electrospun Al_2O_3–SiO_2 nanofibers. Beilstein J Nanotechnol 6:313–320
42. Chaaya AA, Viter R, Baleviciute I, Bechelany M, Ramanavicius A, Gertnere Z, Erts D, Smyntyna V, Miele P (2014) Tuning optical properties of Al_2O_3/ZnO nanolaminates snthesized by atomic layer deposition. J Phys Chem C 118:3811–3819
43. Zou JP, Rendu PL, Musa I, Yang SH, Dan Y, That CT, Nguyen TP (2011) Investigation of the optical properties of polyfluorene/ZnO nanocomposites. Thin Solid Films 519:3997–4003
44. Budrugeac P (2008) Kinetics of the complex process of thermo-oxidative degradation of poly(vinyl alcohol). J Therm Anal Calorim 92:291–296
45. Gilman JW, Van der Hart DL, Kashiwagi T (1994) Fire and polymers II: materials and test for hazard prevention, American Chemical Society, ACS Symposium Series 599, August 21–26, Washington, DC
46. Singh R, Kulkarni SG, Naik NH (2013) Effect of nano sized transition metal salts and metals on thermal decomposition behavior of polyvinyl alcohol. Adv Mater Lett 4:82–88
47. Leszczynska A, Njuguna J, Pielichowski K, Banerjee JR (2007) Polymer/montmorillonite nanocomposites with improved thermal properties: Part I. Factors influencing thermal stability and mechanisms of thermal stability improvement. Thermochim Acta 453:75–96
48. Rahman Khan MM, Wee YK, Mahmood WAK (2014) Effect of CuO on the thermal stability of polyaniline nanofibers. Int J Chem React Eng 12:1–7
49. Lee J, Bhattacharyya D, Easteal AJ, Metson JB (2008) Properties of nano-ZnO/poly(vinyl alcohol)/poly(ethylene oxide) composite thin films. Curr Appl Phys 8:42
50. Radosavljević A, Božanić D, Bibić N, Mitrić M, Popovic ZK, Nedeljković J (2012) Characterization of poly(vinyl alcohol)/gold nanocomposites obtained by in situ gamma-irradiation method. J Appl Polym Sci 125:1244–1251
51. Peresin MS, Habibi Y, Zoppe JO, Pawlak JJ, Rojas OJ (2010) Nanofiber composites of polyvinyl alcohol and cellulose nanocrystals: manufacture and characterization. Biomacromolecules 11:674–681
52. Guo Z, Zhang D, Wei S, Wang Z, Karki AB, Li Y, Bernazzani P, Young DP, Gomes JA, Cocke DL, Ho TC (2010) Effects of iron oxide nanoparticles on polyvinyl alcohol: interfacial layer and bulk nanocomposites thin film. J Nanopart Res 12:2415–2426
53. Chandrakala HN, Ramaraj B, Shivakumaraiah, Madhu GM, Siddaramaiah (2012) The influence of zinc oxide–cerium oxide nanoparticles on the structural characteristics and electrical properties of polyvinyl alcohol films. J Mater Sci 47:8076–8084
54. Soltani N, Saioni E, Yunus WMM, Navasery M, Bahmanrokh G, Erfania M, Reza Zare M, Gharibshahi E (2013) Photocatalytic degradation of methylene blue under visible light using PVP-capped ZnS and CdS nanoparticles. Sol Energy 97:147–154